Mode Transition Induced by Low-Frequency Current in Dual-Frequency Capacitive Discharges

H. C. Kim and J. K. Lee*

Department of Electronic and Electrical Engineering, Pohang University of Science and Technology, Pohang 790-784, Republic of Korea

(Received 21 April 2004; published 19 August 2004)

The mode transition induced by varying the low-frequency current in low-pressure dual-frequency discharges in argon is found through particle-in-cell or Monte Carlo simulations. As the low-frequency (2 MHz) current increases for the fixed high-frequency (27 MHz) current, the electron distribution function (EDF) changes from Druyvesteyn to bi-Maxwellian (in α mode) or Maxwellian-type (in γ mode), along with the significant drop in the effective electron temperature. It is shown that this EDF evolution is attributed to the transition from collisional to collisionless property (but not stochastic heating) of the low-energy electrons as well as the $\alpha - \gamma$ transition.

DOI: 10.1103/PhysRevLett.93.085003 PACS numbers: 52.80.Pi, 52.27.Aj, 52.65.Rr

Capacitively coupled rf discharges have been extensively studied for the last decades because of their interesting physics as well as their widespread applications [1]. Concerning the sustainment of capacitively coupled rf discharges, at least two types of discharge transitions have been reported. One is the transition from collisionless (or non-Ohmic) to collisional (or Ohmic) electron heating with increasing gas pressure [2]. At low pressure, capacitive rf discharges are maintained by collisionless heating. Although the collisionless heating mechanism has been understood as stochastic heating, the alternative mechanism associated with pressure effects [3] has also been proposed. The other type is the transition from the low-voltage (or α) to the high-voltage (or γ) mode with increasing discharge current density [4]. At the low rf discharge voltage the ionization is provided by the bulk plasma electrons, while at the high voltage the ionization is maintained by the secondary electrons from the electrodes due the ion bombardment. Both transitions are accompanied by the changes in the electron distribution function (EDF) and the effective electron temperature ($T_{\text{eff}} = 2\langle\varepsilon\rangle/3$). However, most of the previous works have been limited only to the conventional capacitively coupled plasma (CCP) with a single rf (13.56 MHz) source. Recently, dual-frequency (DF) CCP operated with one more power supply than the conventional CCP has attracted much attention due to its advantage of the independent control of the ion flux and ion bombardment energy onto the electrodes [5–9]. It was found from the numerical simulation [7] that the dependence of the electron temperature on the low-frequency power source plays an important role for the independent control of the ion flux and ion bombardment energy. In spite of widespread practical applications of DF CCP, its physics has not been fully understood.

In this Letter, we report on the mode transition induced by varying the low-frequency current in DF CCP. For this study, we have used a one-dimensional electrostatic particle-in-cell (PIC) simulation method with a Monte Carlo collision model (MCC) [10], which is a self-consistent and fully kinetic method. Our simulations were performed for argon discharges with two parallel-plate electrodes separated by the gap distance of 2.5 cm. Operating gas pressure was 100 mTorr. Two rf current sources with frequencies of 27 MHz ($=w_h$) and 2 MHz ($=w_l$) were applied to the powered electrode at position $x = 0$ cm. The amplitude of the high-frequency (27 MHz) current was fixed at 1 mA cm^{-2}, while the low-frequency (2 MHz) current was varied in the range of 0–0.3 mA cm^{-2}. The electrode at position $x = 2.5$ cm was grounded. In order to obtain the meaningful result in the steady state, we performed the simulation runs for several thousand rf cycles. The secondary electron emission (SEE) coefficients due to the ion impact are different for various electrode materials. Two cases with and without the SEE were simulated.

For the case without the SEE, the EDFs calculated at the discharge center for different low-frequency currents are shown in Fig. 1(a). As the low-frequency current increases, it changes from Druyvesteyn to bi-Maxwellian-type. The temperature of low-energy electrons decreases, while the tail temperature increases. As shown in Fig. 1(b), the effective electron temperature at the discharge center decreases with the low-frequency current along with the small increase of the electron density. The discharge is not sustained for much higher low-frequency current above 0.25 mA cm^{-2} because of the significant decrease of the bulk plasma length [8]. The effective electron temperature is mostly determined by the electrons having energy in elastic range. At the gas pressure of 100 mTorr with the gap distance $2L = 2.5$ cm, since half of the gap distance is much less than the energy relaxation length λ_ε for the electrons in elastic energy range ($\lambda_\varepsilon \gg L$), these electrons are in the nonlocal regime [11]. In this regime, the electrons are trapped by the potential well formed by the ambipolar potential, and the

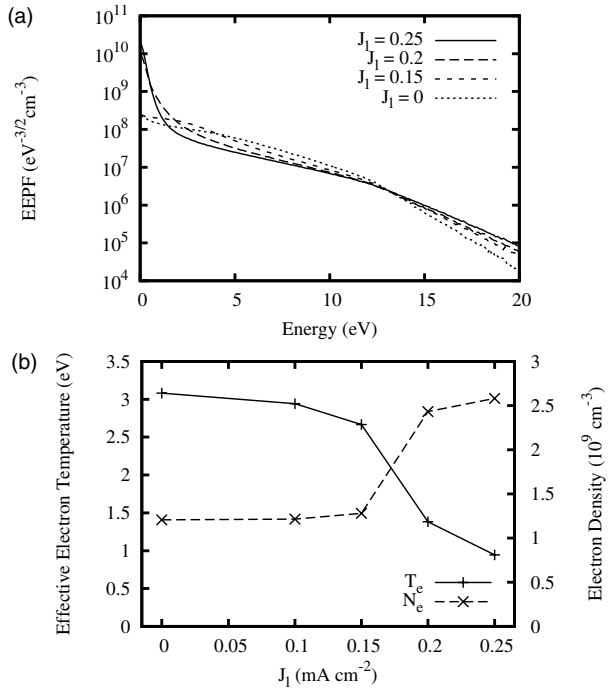

FIG. 1. Simulation result for the mode transition without SEE: (a) Electron energy probability functions at the discharge center for various low-frequency currents. (b) Effective electron temperature and electron density at the discharge center as a function of the low-frequency current. Time-averaged values were presented.

accessible volume of the electrons depends on their energies. The EDF is mainly affected by the spatial inhomogeneity of the electric field, the sheath heating, and the Ramsauer effect [12].

Figure 2(a) shows the time-averaged spatial profiles of the rf electric field for different low-frequency currents. In the sheath region where the displacement current is dominant, the low-frequency field can dominate the high-frequency one. On the other hand, the electric field in the bulk plasma region is typically contributed from the high-frequency field rather than from the low-frequency one. However, because two rf sources are coupled to each other [8], the low-frequency source can affect the high-frequency field. As shown in Fig. 2(a), the electric field at the discharge center decreases with the low-frequency current while the field at the sheath increases. As a result, the temperature of low-energy electrons decreases while the tail temperature increases, as shown in Fig. 1(a). The inhomogeneity of the electric field increases with the low-frequency current. This inhomogeneous electric field structure leads to the bi-Maxwellian EDF since higher-energy electrons are accessible to the regions of higher rf field strength. It is also interesting that the electric field structure is not monotonic near the bulk-sheath boundaries. A similar phenomenon was observed in inductively coupled plasmas by Godyak and Kolobov [13]. However, there is no anomalous skin effect in CCP. This nonmonotonic field structure disappears in our other simulations (not shown here) by removing the Ramsauer minimum in elastic collision cross section. Thus, it is associated with the Ramsauer effect such as the nonmonotonic power deposition structure near the bulk-sheath boundaries of Ref. [14].

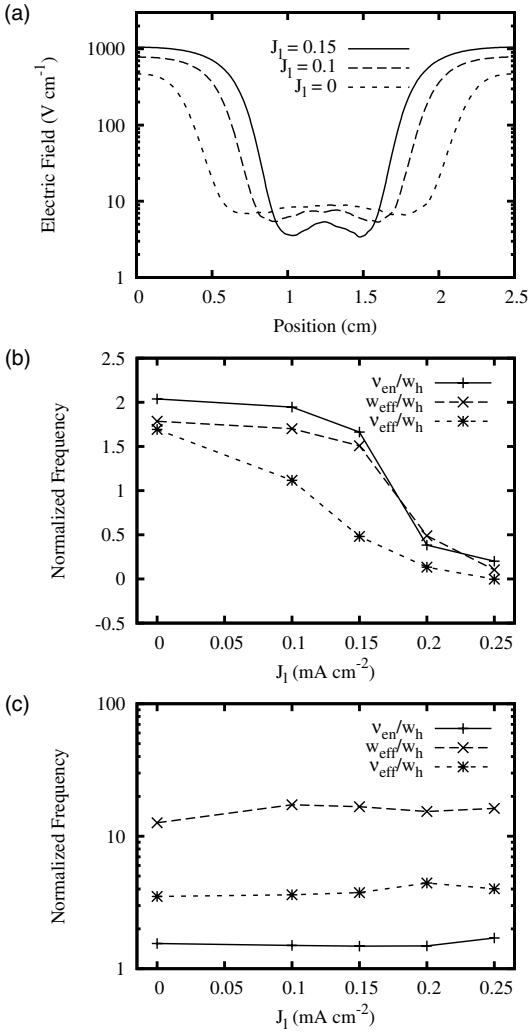

FIG. 2. Simulation result without SEE: (a) The time-averaged spatial profiles of the rf electric field for different low-frequency currents. Frequencies calculated at (b) the discharge center and (c) the position where the consumed power by electrons has the maximum value.

In order to understand how the electric field at the discharge center changes with the low-frequency current, the relation between the rf electric field and rf current density (Ohm's law) is analyzed as follows:

$$\tilde{J} = \sigma_p \tilde{E} \tag{1}$$

with the generalized form of the plasma conductivity

$$\sigma_p = \frac{\varepsilon_0 w_{pe}^2}{\nu_{eff} + j w_{eff}}, \tag{2}$$

where $\varepsilon_0 = 8.85 \times 10^{-12}$ Fm^{-1} and w_{pe} are the permittivity of free space and the electron plasma frequency, respectively. Frequencies ν_m and w are replaced by effective frequencies ν_{eff} and w_{eff}. The collision frequency ν_m is not the same as ν_{eff} when the EDF is not Maxwellian, the collision frequency is not constant for electron energy, or there is significant collisionless (or non-Ohmic) power absorption [15,16]. The values of ν_{eff} and w_{eff} can be obtained from the plasma resistivity [16]

$$\rho = \tilde{E}\cos\psi/\tilde{J} = \mathrm{Re}(\sigma^{-1}) = m\nu_{eff}/ne^2 \qquad (3)$$

and plasma reactance

$$\xi = \tilde{E}\sin\psi/\tilde{J} = \mathrm{Im}(\sigma^{-1}) = mw_{eff}/ne^2, \qquad (4)$$

where m is the electron mass, n is the plasma density, and ψ is the phase shift between the rf electric field $\tilde{E}$ and the rf current density $\tilde{J}$. From the simple analysis of the Boltzmann equation in DF CCP, it can be shown that the EDF in the bulk plasma region is governed by the high-frequency field rather than the low-frequency one. The effective frequencies only for the high-frequency source were calculated by using $\tilde{E}_h$, $\tilde{J}_h$, and ψ_h obtained from the PIC/MCC simulation.

Figures 2(b) and 2(c) show frequencies ν_{en}, w_{eff}, and ν_{eff} at the discharge center and the position of maximum electron power deposition, respectively. All the frequencies were normalized to w_h. According to the generalized Ohm's law of Eq. (1) for the fixed high-frequency current, the change of the electric field is due to that of w_{pe}, ν_{eff}, or w_{eff}. It is noted from the comparison of the plasma density and the effective frequencies [Figs. 1(b) and 2(b)] that the change of the electric field at the discharge center is mainly due to two effective frequencies rather than the plasma density. The significant decrease of the frequencies can be interpreted as the transition from collisional to collisionless property of the low-energy electrons. For the argon gas, the electron mean free path for momentum transfer λ_e between 0.4 and 10 cm decreases with energy because of the Ramsauer minimum. As shown in Fig. 2(a), the plasma width $2d$ decreases with the low-frequency current because of the increase of the sheath width. As a result, the low-energy electrons become collisionless (since $\lambda_e \gg d$) and their temperature significantly decreases. This trend is quite opposite to the result of the global model (volume-averaged fluid model), that the electron temperature increases with the decrease of the plasma width [1]. Unlike the results of Refs. [15,16], it is found from Fig. 2(b) that the values of ν_{eff}/ν_{en} and w_{eff}/w_h at the discharge center can also be smaller than unity, along with their anomalous decreases. Since the effective frequency ν_{eff} includes both of the collisional (ν_{en}) and the collisionless effects, our result ($\nu_{eff} < \nu_{en}$) means that there is a significant collisionless effect which leads to electron cooling in the plasma bulk region. It is consistent with the result of Ref. [3] that the total electron heating at the discharge center is smaller than the Ohmic heating. It can arise from the nonlocal behavior of the electrons since the conductivity in the nonlocal regime has the different form with the classical conductivity [17]. It is therefore concluded that the EDF evolution while changing the low-frequency current is attributed to the transition from collisional to collisionless property of the low-energy electrons. On the other hand, it is found from Fig. 2(c) that the effective frequencies in the region where stochastic heating is possible do not change much with the low-frequency current. Hence, the collisionless mechanism in our simulation is not attributed to stochastic heating, which is the typical type of collisionless electron heating. According to Ref. [3], stochastic heating is not a dominant electron heating mechanism even in 10 mTorr.

The case with the SEE has also been investigated. The SEE coefficient due to ion impact was set to 0.2. The EDFs calculated at the discharge center for different low-frequency currents are shown in Fig. 3(a). As the low-frequency current increases, it changes from Druyvesteyn to Maxwellian type. As shown in Fig. 3(b), the effective electron temperature decreases with the low-frequency current. In comparison with the case without the SEE [Fig. 1(b)], there is a significant increase of the plasma density. The time-averaged spatial

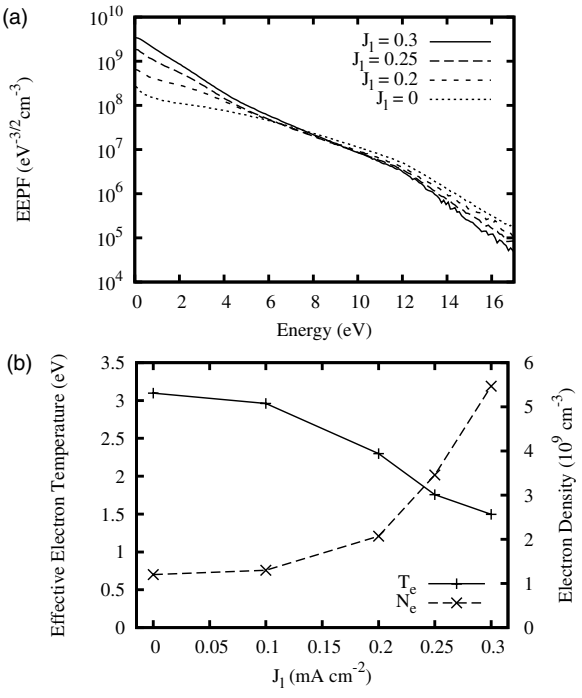

FIG. 3. Simulation result for the mode transition with SEE: (a) Electron energy probability functions at the discharge center for various low-frequency currents. (b) Effective electron temperature and electron density at the discharge center as a function of the low-frequency current.

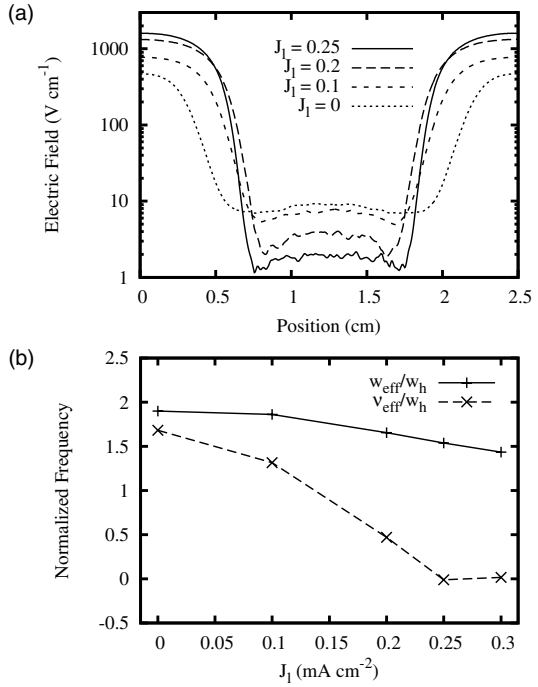

FIG. 4. Simulation result with SEE: (a) The time-averaged spatial profiles of the rf electric field for different low-frequency currents. (b) Frequencies calculated at the discharge center.

profiles of the rf electric field are shown in Fig. 4(a). As the low-frequency current increases, the electric field at the discharge center decreases, and hence the inhomogeneity of the electric field increases. Figure 4(b) shows the effective frequencies w_{eff} and ν_{eff} at the discharge center. Unlike the case without the SEE, it is noted from the comparison of the plasma density and the frequencies [Figs. 3(b) and 4(b)] that the change of the electric field at the discharge center is mainly due to the plasma density rather than the frequencies. From the comparison of two cases with and without the secondary emission, it is noted that the EDF evolution for the case with the SEE is associated with the $\alpha - \gamma$ transition [4]. As the low-frequency current increases, the sheath voltage increases, and hence the SEE due to the ion impact becomes the dominant ionization process. The discharge is changed from the low-voltage to the high-voltage mode.

In conclusion, we have found the mode transition induced by varying the low-frequency current in DF capacitive discharges in argon. As the low-frequency (2 MHz) current increases for the fixed high-frequency (27 MHz) current, the EDF changes from Druyvesteyn to bi-Maxwellian-type (in α mode) or Maxwellian-type (in γ mode), along with the significant drop in the effective electron temperature. The electric field decreases with the low-frequency current, and hence the inhomogeneity of the electric field increases. Depending on the magnitude of the SEE due to the ion bombardment, the mechanism for this EDF change is different. When the role of the SEE is dominant, the EDF evolution while changing the low-frequency current is attributed to the transition from the low-voltage (or α) to the high-voltage (or γ) mode. When the SEE is negligible, the EDF evolution is attributed to the transition from collisional to collisionless property of the low-energy electrons, along with the anomalous decreases of the effective frequencies ν_{eff} and w_{eff}. It was shown that this transition is not related to stochastic heating, which is the typical type of collisionless electron heating.

The authors greatly appreciate helpful discussions with Professor M. A. Lieberman at the University of California at Berkeley and with Dr. N. Yu. Babaeva. This work was supported in part by the LAM Research Corporation, Samsung Electronics, and Korea Ministry of Education through its Brain Korea 21 program.

*Electronic address: jk1@postech.ac.kr

[1] M. A. Lieberman and A. J. Lichtenberg, *Principles of Plasma Discharges and Materials Processing* (Wiley, New York, 1994).
[2] V. A. Godyak and R. B. Piejak, Phys. Rev. Lett. **65**, 996 (1990).
[3] M. M. Turner, Phys. Rev. Lett. **75**, 1312 (1995).
[4] V. A. Godyak, R. B. Piejak, and B. M. Alexandrovich, Phys. Rev. Lett. **68**, 40 (1992).
[5] T. Kitajima, Y. Takeo, Z. L. Petrovic, and T. Makabe, Appl. Phys. Lett. **77**, 489 (2000).
[6] S. Rauf and M. J. Kushner, IEEE Trans. Plasma Sci. **27**, 1329 (1999).
[7] P. C. Boyle, A. R. Ellingboe, and M. M. Turner, J. Phys. D **37**, 697 (2004).
[8] H. C. Kim, J. K. Lee, and J. W. Shon, Phys. Plasmas **10**, 4545 (2003).
[9] J. K. Lee, N. Babaeva, H. C. Kim, O. Manuilenko, and J. W. Shon, IEEE Trans. Plasma Sci. **32**, 47 (2004).
[10] J. P. Verboncoeur, M. V. Alves, V. Vahedi, and C. K. Birdsall, J. Comput. Phys. **104**, 321 (1993).
[11] I. D. Kaganovich and L. D. Tsendin, IEEE Trans. Plasma Sci. **20**, 66 (1992).
[12] U. Buddemeier, U. Kortshagen, and I. Pukropski, Appl. Phys. Lett. **67**, 191 (1995).
[13] V. A. Godyak and V. I. Kolobov, Phys. Rev. Lett. **79**, 4589 (1997).
[14] M. Surendra and D. B. Graves, Phys. Rev. Lett. **66**, 1469 (1991).
[15] G. G. Lister, Y.-M. Li, and V. A. Godyak, J. Appl. Phys. **79**, 8993 (1996).
[16] V. A. Godyak, R. B. Piejak, and B. M. Alexandrovich, J. Appl. Phys. **85**, 3081 (1999).
[17] B. Ramamurthi, D. J. Economou, and I. D. Kaganovich, Plasma Sources Sci. Technol. **12**, 302 (2003).